JOURNAL OF CATALYSIS 131, 412–432 (1991)

The Effect of Phosphate on the Hydrodenitrogenation Activity and Selectivity of Alumina-Supported Sulfided Mo, Ni, and Ni–Mo Catalysts

S. EIJSBOUTS,[1] J. N. M. VAN GESTEL, J. A. R. VAN VEEN, V. H. J. DE BEER, AND R. PRINS[2]

Schuit Institute of Catalysis, Eindhoven University of Technology, P.O. Box 513, 5600 MB Eindhoven, The Netherlands

Received January 31, 1991; revised April 30, 1991

Al_2O_3-supported Mo, Ni, Ni–Mo, and Rh catalysts, prepared by sequential aqueous impregnation and *in situ* sulfidation, were investigated in the hydrodenitrogenation (HDN) of quinoline at 643 K and 3 MPa and in the hydrodesulfurisation (HDS) of thiophene at 673 K and 0.1 MPa. The Ni and Mo catalysts had a very low conversion of quinoline to hydrocarbons which improved only slightly in the presence of phosphate. The Rh catalysts had a high conversion and a high selectivity for propylcyclohexane and showed no deactivation with time. The addition of Ni to Mo/Al_2O_3 and of phosphate to $Ni–Mo/Al_2O_3$ and Rh/Al_2O_3 catalysts increased the HDN conversion significantly. The selectivity for propylbenzene and the apparent HDN activation energy increased with increasing P-loading. Ni increased the thiophene conversion of Mo/Al_2O_3, but phosphate had almost no influence on the HDS activity of $Ni–Mo/Al_2O_3$ and Rh/Al_2O_3. The effect of phosphate is due to a combination of structural and catalytic factors. Phosphate improves the activity by inducing the formation of the type II Ni–Mo–S structure, but also, especially at high Ni loading, lowers the activity by inducing a decrease in the dispersion of the Ni–Mo–S phases and a segregation of Ni_3S_2. Phosphate also promotes the S- and N-elimination reactions, but this only has an influence on the overall catalyst activity if the preceding hydrogenation reactions are not rate determining. © 1991 Academic Press, Inc.

INTRODUCTION

Commercial hydrodenitrogenation (HDN) catalysts for the treatment of heavy feedstocks usually contain Ni, Mo, and P (*1–5*). While Ni is generally known to function as a promoter for the Mo catalyst (*6*), the role of phosphorus has long been seen as restricted to the enhancement of the solubility of molybdate in the impregnation solution (*3, 5, 7*), and to the improvement of the mechanical and thermal stability of the support by $AlPO_4$ formation (*3, 10*). As to its direct role in HDN or hydrodesulfurisation (HDS) catalysis, there is conflicting patent and other literature, although positive effects on HDS (*3, 4, 7, 9, 11–13*), HDN (*4, 5, 7, 11, 14*), and hydrodemetallation (*4*) have been reported. There have been some attempts to explain these positive effects by changes in active phase dispersion (*9, 13, 14*). It is well known that phosphate has a strong interaction with the Al_2O_3 support (*14–18*) and forms $AlPO_4$ which decreases the adsorption of molybdate (*15*) and weakens the interaction between molybdenum and nickel oxide and the support (*14, 15, 19*). Consequently, the dispersion of the active phase may change. But besides the dispersion, the surface structure and crystal morphology of the catalyst may also change. Thus metal sulfide catalysts have a higher intrinsic activity on less polar supports like carbon (*20–23*), and a high-resolution trans-

[1] Present address: AKZO Research Centre Amsterdam, P.O. Box 15, 1000 AA Amsterdam, The Netherlands.

[2] Present address: Technisch Chemisches Laboratorium, ETH, 8092 Zürich, Switzerland.

0021-9517/91 $3.00
Copyright © 1991 by Academic Press, Inc.
All rights of reproduction in any form reserved.

mission electron microscopy study showed that nickel and phosphate contribute to stacking of the MoS_2 slabs in sulfided Ni–Mo–P/Al_2O_3 catalysts (*24*). It is not clear if this stacking is related to the structure transformation of Co–Mo/Al_2O_3 catalysts described by Candia *et al.* (*25*). By comparing activity data with ^{57}Co Mössbauer emission data they observed that Co–Mo/Al_2O_3 catalysts sulfided at high temperature were intrinsically more active per Co atom in the so-called Co–Mo–S phase (*26*) than those sulfided at normal temperatures (673–773 K). They introduced the notation of type I Co–Mo–S for the Co–Mo–S structure which is formed after low-temperature sulfidation, and type II for the Co–Mo–S structure formed after high-temperature sulfidation. In addition to changing the dispersion and morphology of the active Ni–Mo–S phase, phosphate may also be more directly involved in the HDS or HDN catalysis, for instance in the acid-catalyzed N-removal elimination reaction. In this relation it has been observed that phosphate changes the acidity of the alumina support (*2, 8, 14, 16*), affects the cracking and isomerization activity of the catalyst (*2, 15*), and decreases the formation of coke (*8*).

So to try and unravel the complex role of phosphate in supported Ni-promoted molybdenum sulfide catalysts we have studied the effect of phosphate on the activity and selectivity of sulfided Al_2O_3-supported Ni, Mo, and Ni–Mo catalysts, and Rh catalysts to check on the generality of the observed effects in the HDN of quinoline and in the HDS of thiophene. Two series of Ni–Mo catalysts were employed, both with a Mo loading slightly less than the adsorption capacity of the Al_2O_3 used, but one with a Ni/Mo atomic ratio low enough (0.24) for all Ni to be incorporated in the Ni–Mo–S phase, and the other, seeing that in commercial catalysts more Ni is present than can be accommodated in the Ni–Mo–S phase, with the high ratio of 0.72. In addition, two Ni–Mo/Al_2O_3 catalysts, with and without P, prepared by coimpregnation in the presence of the complexing agent nitrilotriacetic acid (NTA), were studied. NTA-prepared Co–Mo and Ni–Mo catalysts contain Co or Ni almost exclusively in the Co–Mo–S (or Ni–Mo–S) type II structure (*23*) and such catalysts thus may allow us to find out if phosphate induces type I to type II structure transformations. Dual bed experiments, with a bed of P/Al_2O_3 downstream of the Ni–Mo/Al_2O_3 bed, were performed to study the catalytic activity of phosphate on alumina for N-removal reactions subsequent to the initial hydrogenation of quinoline.

We chose to study the HDN of quinoline because it has been studied in detail by Shih *et al.* (*27*), Satterfield and co-workers (*28–33*), Gioia and Lee (*34*), and Schulz *et al.* (*35*). The reaction network is presented in Fig. 1. It consists of several hydrogenation steps, indicated by arrows, and steps in which C–N bonds are broken, indicated by broken arrows. In the main reaction pathway quinoline (Q) is hydrogenated to 1,2,3,4-tetrahydroquinoline (THQ1) and 5,6,7,8-tetrahydroquinoline (THQ5) and on to decahydroquinoline (DHQ). Thereafter, elimination or hydrogenolysis reactions open the N-containing ring of DHQ and finally remove the N atom. The final product consists of a mixture of propylbenzene (PBZ), propylcyclohexane (PCH), and propylcyclohexene (PCHE). The advantage of quinoline over other N-containing molecules is that both the hydrogenation and the N-removal steps are important for the kinetics, because the formation of DHQ as well as the breaking of the C–N bond in DHQ are slow steps (*27, 31, 33*). For aniline (*35, 36*) and pyrrole (*35*) the primary hydrogenation is rate determining so nothing can be learned about the C–N bond breaking. In the HDN of pyridine, on the other hand, by-products are formed through reactions of intermediate alkenes with amines (*35, 37 38*). These by-products, which are also formed in the HDN of aniline (*36*) and pyrrole (*35*), complicate the analysis of the main HDN network. Since these side reactions are almost nonexistent with quinoline, we have chosen quinoline as a model compound in the study of the influence of phosphate on

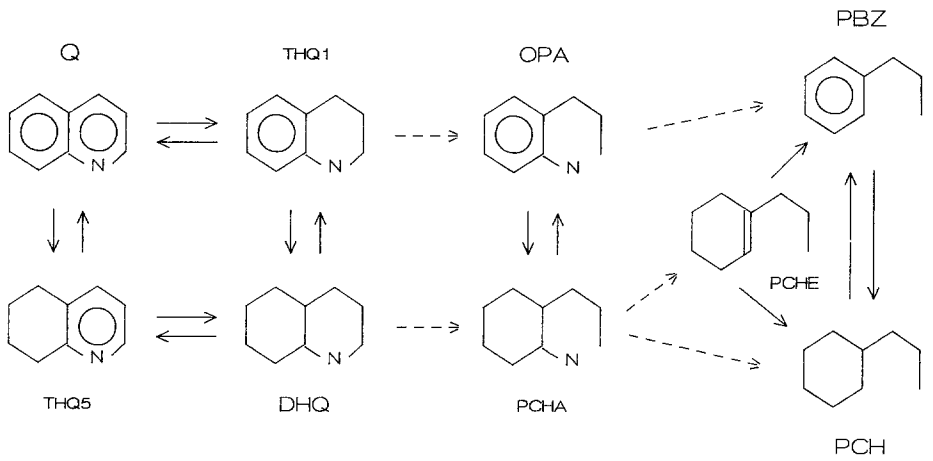

FIG. 1. Reaction network of the HDN of quinoline. Q, quinoline; THQ1, 1,2,3,4-tetrahydroquinoline; THQ5, 5,6,7,8-tetrahydroquinoline; DHQ, decahydroquinoline; OPA, *o*-propylaniline; PCHA, propylcyclohexylamine; PCHE, propylcyclohexene; PBZ, propylbenzene; PCH, propylcyclohexane.

the activity and selectivity of Ni–Mo HDN catalysts.

EXPERIMENTAL

Catalysts

Phosphate-containing catalysts were prepared by sequential impregnation of the γ-Al_2O_3 support (Ketjen 001–1.5E, Al_2O_3 > 97.3 wt%, surface area 280 m^2g^{-1}, pore volume 0.67 cm^3g^{-1}, particle diameter 0.2–0.5 mm) with aqueous solutions of *o*-H_3PO_4, $(NH_4)_6Mo_7O_{24} \cdot 4H_2O$ and $Ni(NO_3)_2 \cdot 6H_2O$, or respectively $RhCl_3$ and *o*-H_3PO_4 (all Merck, p.a.). Phosphate-free catalysts were prepared analogously. After each impregnation step the catalysts were slowly heated over a period of 3 h from 293 to 383 K and then dried for 16 h in static air at 383 K. All catalysts were calcined in air at 823 K (temperature increased from 293 to 823 K in 1 h, 1 h at 823 K) after the last impregnation step. The P–Rh catalyst was calcined after both impregnation steps. A P-free and a P-containing $Ni(0.6)Mo/Al_2O_3$ catalyst were prepared via the NTA route (NTA, nitrilotriacetic acid) (*23*). For these two catalysts a different commercial γ-Al_2O_3 (SA = 250 m^2g^{-1}, PV = 0.75 cm^3g^{-1}) was used and the phosphorus was introduced as $NH_4H_2PO_4$ onto the support through adsorption. After drying and calcining, a pore volume impregnation with an aqueous solution containing the required amounts of Ni, Mo and NTA (NTA/Mo = 1.2) was applied. The NTA catalysts were only dried, not calcined, before sulfidation. The composition of the oxidic precursor catalyst systems, together with their surface area and pore volume, are listed in Table 1. In the text the following notation is used: $*Ni(x)MoP(y)/Al_2O_3$, where x and y are the loadings in atoms per square nanometers of the original support surface. The Mo loading of all Mo-containing catalysts was about 2.1 at. nm^{-2}. The elements are ordered according to the sequence of impregnation, starting from the support. The asterisk indicates after which impregnation step the calcination took place. The composition of the catalysts was determined by atomic absorption spectroscopy and UV–VIS spectroscopy (Table 1). The catalysts have also been characterised by means of temperature-programmed desorption of NH_3 and BET measurements.

Quinoline HDN

A 0.5-g catalyst sample was diluted with 9.5 g SiC and sulfided *in situ* using a flow of 150 std cm^3 min^{-1} of a mixture containing 10

TABLE 1

Catalyst Composition and Texture

Catalyst[a]	Ni (wt%)	Mo (wt%)	P (wt%)	SA[b] (m^2g^{-1})	PV[b] (cm^3g^{-1})
*Al_2O_3	—	—	—	280	0.67
*P(4)/Al_2O_3	—	—	5.2	—	—
$AlPO_4$	—	—	21.5	240	2.1
*Ni(1.5)/Al_2O_3	3.3	—	—	—	—
*Ni(1.5)P(4)/Al_2O_3	3.2	—	4.2	—	—
*Mo/Al_2O_3	—	7.0	—	—	—
*MoP(4)/Al_2O_3	—	6.8	4.2	—	—
*Ni(1.5)Mo/Al_2O_3	3.4	7.7	—	237 (232)	0.53 (0.56)
*Ni(1.5)MoP(0.5)/Al_2O_3	3.5	7.9	0.7	—	—
*Ni(1.5)MoP(1)/Al_2O_3	3.0	8.1	1.2	219 (212)	0.47 (0.53)
*Ni(1.5)MoP(2)/Al_2O_3	3.1	7.3	2.1	198 (209)	0.46 (0.51)
*Ni(1.5)MoP(4)/Al_2O_3	3.1	7.1	4.4	151 (188)	0.38 (0.46)
*Ni(1.5)MoP(6)/Al_2O_3	2.8	6.7	6.2	108 (167)	0.31 (0.41)
*Ni(0.5)Mo/Al_2O_3	1.2	7.9	—	—	—
*Ni(0.5)MoP(0.5)/Al_2O_3	1.2	7.4	0.6	—	—
*Ni(0.5)MoP(2)/Al_2O_3	1.1	7.5	2.3	—	—
*Ni(0.5)MoP(4)/Al_2O_3	1.1	6.7	4.3	—	—
[Ni(0.6)Mo + NTA]/Al_2O_3	1.4	7.3	—		
[Ni(0.6)Mo + NTA]P(2)/Al_2O_3	1.4	7.3	1.9		
*Rh(0.5)/Al_2O_3	2.2 (Rh)		—		
*P(1)*Rh(0.5)/Al_2O_3	2.2 (Rh)		1.1		

[a] For catalyst notation see section Experimental, Catalysts.

[b] SA, surface area; PV, pore volume. Both values are related to 1 g of catalyst. The values in parentheses are calculated based on the assumption that all phosphate is present as $AlPO_4$ and that $AlPO_4$, NiO, and MoO_3 have no contribution to the SA and PV.

vol% H_2S in H_2 (Air Products, $H_2 > 99.99\%$, $H_2S > 99.9\%$). The temperature was increased (6 K min^{-1}) to 643 K and held at this level for 4 h, and the pressure was 1.5 MPa. After the sulfidation the reactor pressure was increased to 3.0 MPa and 12 μl min^{-1} of liquid feed (composition: 23.8 mol% Q (Janssen Chimica 99%), 3.8 mol% dimethyldisulfide (DMDS) (Fluka 99%) and 72.4 mol% decane (Janssen Chimica > 99%)) evaporated in 950 std cm^3 min^{-1} H_2 (Hoekloos 99.99%) was led through the reactor (LHSV = 2×10^{-3} mol Q h^{-1} g^{-1} catalyst, GHSV = 5 mol H_2 h^{-1} g^{-1} catalyst). The reaction mixture was analysed each hour. When a constant activity was reached (in general after about 18 h on stream), the reaction temperature was increased to 663 K, held for 3 h, decreased to 623 K, held for 3 h, and then increased to 643 K and held again for 3 h. The reactant mixture was analysed on line using a Hewlett–Packard 5890A GC equipped with a 50-m capillary CP Sil-5 fused silica column (Chrompack, i.d. 0.22 mm, film thickness 0.2 μm) used with temperature programming, a flame ionisation detector, and a nitrogen–phosphorus detector.

In addition to these experiments with 0.5 g catalyst diluted with 9.5 g SiC HDN experiments with combined beds were also carried out in which a second bed of 0.5 g Al_2O_3, *P(4)/Al_2O_3, or $AlPO_4$ diluted with 1.5 g SiC was placed downstream of the catalyst bed. The $AlPO_4$ was prepared according to the procedure of Campelo *et al.* (*39*) by mixing aqueous solutions of $AlCl_3 \cdot 6H_2O$ and H_3PO_4 in stoichiometric amounts

in the presence of ammonia, the final pH of precipitation being 6.1. The precipitate was washed with isopropylalcohol, dried at 393 K for 24 h, and calcined at 920 K for 3 h. Properties of the resulting $AlPO_4$ are given in Table 1.

In the experiments with the NTA catalysts 0.625 g of the dried catalyst was used, since the NTA decomposes upon sulfidation and the resulting fragments desorb from the catalyst (*40*). A 0.625-g sample of a fresh NTA catalyst, after sulfidation, is equivalent to a 0.5-g NTA-free catalyst. To keep the NTA decomposition under control the temperature increase during sulfidation was performed at a lower rate (2 instead of 6 K min^{-1}) and the final sulfidation temperature of 623 K was held for 3 h.

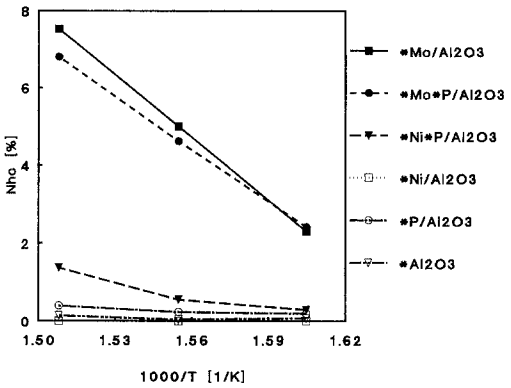

FIG. 2. Quinoline conversion to hydrocarbons, N_{hc} in percentage, versus $1000/T$ of *Mo/Al_2O_3, *MoP(4)/Al_2O_3, *Ni(1.5)/Al_2O_3, *Ni(1.5)P(4)/Al_2O_3, *P(4)/Al_2O_3, and Al_2O_3.

Thiophene HDS

The thiophene HDS experiments have been carried out in the gas phase in a microflow reactor with on-line GC analysis. A 0.2-g catalyst sample was sulfided *in situ* using a mixture of 10% H_2S in H_2 (60 std cm^3 min^{-1}, 6 K min^{-1} from 293 to 673 K, 2 h at 673 K, 0.1 MPa). After that, the reaction mixture consisting of 6.2 vol% thiophene in H_2 was led through the reactor (50 std cm^3 min^{-1}, 2 h, 673 K, 0.1 MPa) and was analysed on line every 15 min. The first-order reaction rate constants for thiophene conversion to hydrocarbons (k_{hds}) and the consecutive hydrogenation of butenes (k_{hydr}) were calculated using activity data after 2 h on stream (steady state) (*41, 42*). As no other S-containing compounds, besides thiophene and H_2S, were found in the reaction product mixture, the thiophene conversion to hydrocarbons is further referred to as thiophene conversion. To compensate for the NTA present in the fresh catalysts 0.25 g of the NTA catalysts was used and during sulfidation these catalysts were heated at 2 K min^{-1} to 623 K and further sulfided at that temperature for only 1 h.

XPS

The XPS measurements were carried out on oxidic and sulfided catalysts using the same procedure and settings as described previously (*21*), except for the sulfiding procedure, which was the same as the one used for the HDN experiments (10% H_2S in H_2, 150 std cm^3 min^{-1}, 6 K min^{-1} from 293 to 643 K, 4 h at 643 K, 1.5 MPa). After the sulfidation was finished the catalysts were flushed with He at 643 K for 15 min and rapidly cooled to room temperature in the He atmosphere. The closed reactor was transferred to a N_2 purged glove box (O_2 and $H_2O < 2$ ppm), the catalyst sample was placed in a Pyrex tube, which was then sealed. The transfer of the samples on the XPS sample holder and the transport of the holder into the spectrometer also took place in an N_2-purged glove box.

For the oxidic catalysts the following elements have been scanned: Ni 2*p*, Mo 3*d*, Rh 3*d*, P 2*p*, and 2*s*, Al 2*p*, and O 1*s*. Intensity ratios to be presented are based on the following peak areas: Ni $2p_{1/2+3/2}$, Mo $3d_{3/2+5/2}$, Al 2*p*, P 2*p*, and Rh $3d_{3/2+5/2}$. Peaks of C 1*s*, In 3*d*, and N 1*s* have been used as internal standards for binding energy calibration. For the sulfided samples the Ni $2p_{1/2}$ peak could not be measured. The area of the Ni $2p_{1/2}$ peak has therefore been calculated from the $2p_{3/2}$ peak using the sensitivity factors 14.61 for Ni $2p_{3/2}$ and 7.57 for Ni $2p_{1/2}$ (*43*). In addition to the elements measured in the XPS of the oxidic

TABLE 2A

Quinoline HDN (643 K, 3 MPa)

Catalyst[a]	Product composition[b]									
	N_{hc}	N_{pch}	N_{pbz}	N_{pche}	N_{dhq}	N_{thq5}	N_q	N_{thq1}	N_{opa}	N_{by}
*Al_2O_3	0.0	0.0	0.0	0.0	0.0	0.8	45.4	53.6	0.0	0.1
*P(4)/Al_2O_3	0.2	0.0	0.0	0.1	2.2	1.3	25.9	68.3	0.3	1.8
$AlPO_4$	0.0	0.0	0.0	0.0	1.0	2.0	24.7	71.0	0.2	1.0
*Ni(1.5)/Al_2O_3	0.0	0.0	0.0	0.0	1.5	6.8	17.8	73.4	0.5	0.0
*Ni(1.5)P(4)/Al_2O_3	0.5	0.1	0.1	0.3	4.0	11.4	17.4	63.8	0.5	2.3
*Mo/Al_2O_3	5.0	1.9	1.8	1.4	5.6	19.9	15.0	49.6	4.9	0.0
*MoP(4)/Al_2O_3	4.6	1.3	1.9	1.4	7.3	20.6	15.2	45.9	3.6	2.8
*Ni(1.5)Mo/Al_2O_3	23.2	15.2	5.6	2.6	10.5	36.3	5.8	19.6	4.0	0.5
*Ni(1.5)MoP(0.5)/Al_2O_3	29.1	18.8	7.3	3.0	9.3	30.7	7.1	18.4	4.4	0.9
*Ni(1.5)MoP(1)/Al_2O_3	34.5	22.1	8.9	3.5	9.4	29.2	5.5	15.6	4.5	1.2
*Ni(1.5)MoP(2)/Al_2O_3	42.8	26.9	11.7	4.2	8.2	25.4	4.8	12.8	4.6	1.4
*Ni(1.5)MoP(4)/Al_2O_3	42.1	25.9	11.1	5.1	8.4	24.3	6.1	13.1	4.4	1.6
*Ni(1.5)MoP(6)/Al_2O_3	42.9	25.3	12.2	5.3	7.8	25.7	4.2	12.7	3.1	3.7
*Ni(0.5)Mo/Al_2O_3	12.4	6.5	3.0	2.9	8.3	34.9	10.6	29.0	4.7	0.0
*Ni(0.5)MoP(0.5)/Al_2O_3	16.2	8.1	4.2	3.4	6.4	29.5	14.4	25.6	3.9	3.9
*Ni(0.5)MoP(2)/Al_2O_3	19.8	9.6	5.6	4.6	9.7	29.4	9.3	26.9	4.5	0.5
*Ni(0.5)MoP(4)/Al_2O_3	22.4	10.1	7.1	5.2	8.7	30.0	8.8	21.8	4.6	3.7
[Ni(0.6)Mo + NTA]/Al_2O_3	34	20	9	4	5	31	8	16	3	2
[Ni(0.6)Mo + NTA]P(2)/Al_2O_3	69	44	19	5	1	14	4	5	2	4
*Rh(0.5)/Al_2O_3	18.4	17.2	1.0	0.2	12.2	39.7	6.8	19.0	2.1	1.8
*P(1)*Rh(0.5)/Al_2O_3	29.4	26.6	2.4	0.4	11.0	36.1	6.1	12.9	2.1	2.5

[a] For catalyst notation see Catalysts section under Experimental.

[b] N_x is the conversion of Q to product x (in %). n_x is the selectivity for compound x (in %), $n_x = N_x/N_{hc}$ for hydrocarbons and $n_x = N_x/N_n$ for the double ring N compounds. For abbreviations see Fig. 1.

$$N_{pch} + N_{pbz} + N_{pche} = N_{hc}$$
$$N_{dhq} + N_{thq5} + N_q + N_{thq1} = N_n$$
$$N_{hc} + N_n + N_{opa} + N_{by} = 100$$

catalysts, in the XPS of the sulfidic samples also the S 2*p* peak has been scanned. The error in the determination of the XPS intensity ratios was approximately 15%.

RESULTS

Quinoline HDN

*Al_2O_3, *Ni/Al_2O_3, and *Mo/Al_2O_3.* The Al_2O_3 support and the *Ni(1.5)/Al_2O_3 and *Mo/Al_2O_3 catalysts had a low conversion of Q to hydrocarbons (N_{hc}) and to cracking and isomerisation products (N_{by}), which increased somewhat when phosphate was added (Fig. 2, Table 2A, 2B). The selectivities for THQ1 (n_{thq1}) and PCHE (n_{pche}) decreased and those for DHQ (n_{dhq}) and THQ5 (n_{thq5}) increased with increasing N_{hc}, as is to be expected on the basis of the work of Satterfield *et al.* (*29–33*) for the consecutive reaction network (cf. Fig. 1). As the reactor effluent stream could not be cooled fast enough below 473 K, the Q–THQ1 equilibrium adjusted to the lower temperature and the product mixture contained more THQ1 than corresponding to the reaction temperature for all catalysts from this series, with the exception of Al_2O_3.

*$Ni(1.5)MoP(0–6)/Al_2O_3$. The Q-conversion to hydrocarbons (N_{hc}) of the *Ni(1.5)Mo/Al_2O_3 catalyst was much higher

TABLE 2B

Quinoline HDN (643 K, 3 MPa)

Catalyst[a]	Product distribution of hydrocarbons and double-ring N compounds[b]						
	N_{hc}	N_n	n_{pch}/n_{pbz}	n_{pche}	n_{dhq}	n_{thq5}	n_{thq1}
*Al_2O_3	0.0	100	—	—	0	1	54
*$P(4)/Al_2O_3$	0.2	98	—	—	2	1	70
$AlPO_4$	0.0	99	—	—	1	2	72
*$Ni(1.5)/Al_2O_3$	0.0	99	—	—	2	7	74
*$Ni(1.5)P(4)/Al_2O_3$	0.5	97	0.7	57	4	12	66
*Mo/Al_2O_3	5.0	90	1.1	27	6	22	55
*$MoP(4)/Al_2O_3$	4.6	89	0.7	30	8	23	52
*$Ni(1.5)Mo/Al_2O_3$	23	72	2.7	11	14	50	27
*$Ni(1.5)MoP(0.5)/Al_2O_3$	29	66	2.6	10	14	47	28
*$Ni(1.5)MoP(1)/Al_2O_3$	34	60	2.5	10	16	49	26
*$Ni(1.5)MoP(2)/Al_2O_3$	43	51	2.3	10	16	50	25
*$Ni(1.5)MoP(4)/Al_2O_3$	42	52	2.3	12	16	47	25
*$Ni(1.5)MoP(6)/Al_2O_3$	43	50	2.1	12	15	51	25
*$Ni(0.5)Mo/Al_2O_3$	12	83	2.1	23	10	42	35
*$Ni(0.5)MoP(0.5)/Al_2O_3$	16	76	1.9	21	9	39	34
*$Ni(0.5)MoP(2)/Al_2O_3$	20	75	1.7	23	13	39	36
*$Ni(0.5)MoP(4)/Al_2O_3$	22	69	1.4	23	13	43	31
$[Ni(0.6)Mo+NTA]/Al_2O_3$	34	60	2.2	13	8	52	27
$[Ni(0.6)Mo+NTA]P(2)/Al_2O_3$	69	24	2.3	7	3	58	21
*$Rh(0.5)/Al_2O_3$	18	78	17	1	16	51	24
*$P(1)*Rh(0.5)/Al_2O_3$	29	66	11	1	17	55	20

[a] For notation see Catalysts section under Experimental.
[b] See Table 2A for abbreviations.

than the sum of the conversions of the separate *$Ni(1.5)/Al_2O_3$ and *Mo/Al_2O_3 catalysts (Table 2A, 2B). Phosphate increased the Q-conversion to hydrocarbons (N_{hc}) and changed the selectivity of Ni–Mo–P/Al_2O_3 catalysts to a great extent (Table 2A, 2B) but had no effect on the deactivation pattern. The increase in N_{hc} with P-loading levelled off at 2 P at. nm^{-2} (Fig. 3). Interestingly, even a high P-loading of 6 P at. nm^{-2} had no negative effect on the catalyst activity, in contrast to what has been reported for the HDS activity of some Al_2O_3-supported catalysts (*11, 44*). The Q-conversion to hydrocarbons of the catalysts with a high P-loading increased faster with temperature than those of the catalysts with a low P-loading (Fig. 3); i.e., the apparent activation energy increases with P-loading. While a decrease of the liquid and gas hourly space velocities at constant H_2/Q ratio increased both N_{hc} and n_{pch}, N_{hc} increased but n_{pch} decreased with increasing P-loading at constant liquid and gas space velocities (Fig. 4). Not only the Q-conversion to hydrocarbons but also the Q-cracking and isomerization (N_{by}) increased in the presence of phosphate, while the selectivity for OPA (N_{opa}) was more or less unaffected by phosphate.

Although the N_{hc} levelled off at 2 P at. nm^{-2}, the selectivity for PBZ (n_{pbz}) continued to increase and that for PCH (n_{pch}) continued to decrease at higher P-loadings (Table 2A, 2B). PBZ was thus formed preferentially and the n_{pch}/n_{pbz} ratio, which was already much lower than the equilibrium value of 9 (*28*) for the P-free catalyst, decreased even further with increasing P-load-

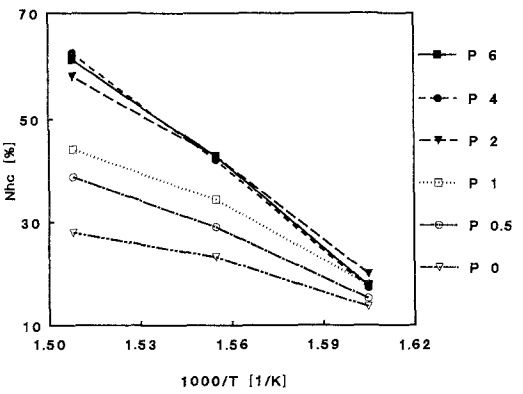

FIG. 3. Quinoline conversion to hydrocarbons, N_{hc} in percentage, versus 1000/T of *Ni(1.5)MoP(0–6)/Al_2O_3 catalysts.

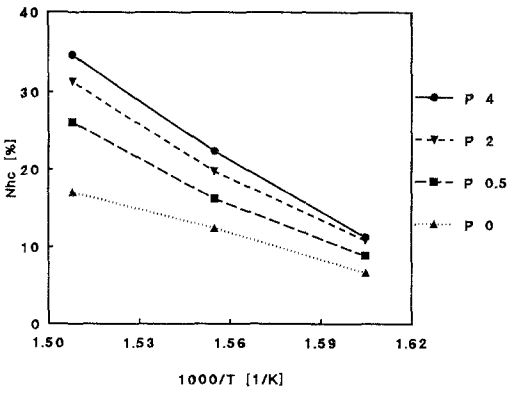

FIG. 5. Quinoline conversion to hydrocarbons, N_{hc} in percentage, versus 1000/T of *Ni(0.5)MoP(0–4)/Al_2O_3 catalysts.

ing. At constant conversion (these data are not given in Table 2) the P-containing catalysts always had a selectivity slightly lower for DHQ and THQ5, and a THQ1 and Q selectivity higher than that of the P-free catalyst. At constant space time the reverse trend was observed (Table 2).

To compare the properties of our catalysts with those of a commercial catalyst, the HDN conversion and selectivity of a commercial Ni(1.5)Mo(3)P(2.6)/Al_2O_3 catalyst were measured under the same conditions as our Ni(1.5)MoP/Al_2O_3 catalysts.

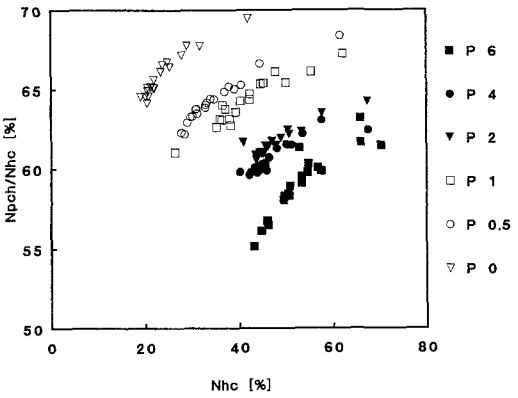

FIG. 4. Selectivity for propylcyclohexane, n_{pch} in percentage, versus quinoline conversion to hydrocarbons, N_{hc} in percentage of *Ni(1.5)MoP(0–6)/Al_2O_3 catalysts at 643 K and varying space time.

The conversion and product distribution were very close to those of the Ni(1.5) MoP(2–4)/Al_2O_3 catalysts, demonstrating that the results obtained with our catalysts are realistic.

*$Ni(0.5)MoP(0–4)/Al_2O_3$. The results of this series of experiments were very similar to those of the previous series. N_{hc} increased with P-loading and levelled off at 2 P at. nm^{-2} (Fig. 5, Table 2A, 2B). Also here no negative effect of phosphate on N_{hc} was found at high P-loading. The relative increase of the N_{hc} was similar (about 80%), as in the high Ni-loading catalyst series. The Q-cracking and isomerisation (N_{by}) increased but the selectivity for OPA did not change in the presence of phosphate. The selectivity for PCH (n_{pch}) decreased and that for PBZ (n_{pbz}) increased with P-loading, even though the N_{hc} levelled off at constant space time. At constant N_{hc}, the selectivity for PCHE increased with P-loading. The selectivity for DHQ (n_{dhq}) increased somewhat with increasing P-loading, but the selectivities for compounds with a hydrogenated benzene ring (n_{dhq}, n_{thq5}) were lower than the equilibrium values.

NTA catalysts. The two NTA catalysts had an N_{hc} much higher than that of the Ni(0.5)MoP/Al_2O_3 catalysts and a different product distribution. The P-containing NTA

TABLE 3

Quinoline HDN (643 K, 3 MPa) of Combined Catalyst Beds

	N_{hc}	N_{pch}	N_{pbz}	N_{pche}	N_{dhq}	N_{thq5}	N_{opa}	N_q	N_{thq1}	N_{by}
*Ni*Mo/Al_2O_3	19	13	4	2	11	32	3	11	24	1
*Ni*Mo/Al_2O_3 + Al_2O_3	19	12	4	3	6	37	3	10	24	1
*Ni*Mo/Al_2O_3 + *P(4)/Al_2O_3	24	15	6	3	3	34	3	13	20	3
*Ni*Mo/Al_2O_3 + $AlPO_4$	24	16	6	2	3	32	3	16	21	2

catalyst even had the highest N_{hc} of all catalysts (Table 2). This very active catalyst with relatively low Ni loading had a low selectivity for OPA, a low cracking and isomerisation activity, and a low conversion of Q to THQ1 and especially to DHQ.

Combined catalyst beds. Experiments with combined catalyst beds consisting of an upstream *Ni*Mo/Al_2O_3 catalyst and a downstream *P(4)/Al_2O_3 or $AlPO_4$ catalyst were carried out in order to see whether the effect of phosphate on the Q–HDN is completely or partly due to the activity of $AlPO_4$ formed on the Al_2O_3 support. For these experiments a new batch of *Ni*Mo/Al_2O_3 catalyst was made, which had a slightly different catalyst composition and texture as the *Ni(1.5)Mo/Al_2O_3 catalyst described before. The Ni and Mo contents of this catalyst were 3.0 and 8.1 wt%, respectively, and SA = 233 $m^2 g^{-1}$ and PV = 0.50 $cm^3 g^{-1}$. Its Q-conversion to hydrocarbons (Table 3) is somewhat lower than that of the *Ni(1.5)Mo/Al_2O_3 catalyst (Table 2), probably because of the lower Ni contents. To check for artifacts in the performance of a second bed downstream of the *Ni*Mo/Al_2O_3 bed, an experiment was done with pure Al_2O_3 as second bed. But the results were very similar to those of the *Ni*Mo/Al_2O_3 catalyst (Table 3) if it is taken into account that, although there was a decrease of n_{dhq} and an increase of n_{thq5}, their sum remained constant.

The catalytic performance of the combined *Ni*Mo/Al_2O_3 + *P(4)/Al_2O_3 bed was significantly different from that of the *Ni*Mo/Al_2O_3 catalyst (Table 3), even though *P(4)/Al_2O_3 had a negligible Q-conversion (Table 2). The Q-conversion to hydrocarbons, as well as the Q-cracking and isomerisation increased at all three measuring temperatures (Fig. 6). At 643 K the N_{hc} increase amounted to 26%. The most significant product changes were the increase in N_{pch} and the decrease in N_{dhq}. The results with a combined *Ni*Mo/Al_2O_3 + $AlPO_4$ bed were very similar to those with *Ni*Mo/Al_2O_3 + *P(4)/Al_2O_3 (Table 3).

Rh/Al_2O_3. Just as for the carbon-supported catalysts (*45, 46*), the Q-conversion to hydrocarbons (N_{hc}) of the *Rh(0.5)/Al_2O_3 catalyst was much higher than those of *Ni(1.5)/Al_2O_3 and *Mo(2.1)/Al_2O_3. Both Rh-containing catalysts showed no deactivation and no changes of product distribution of double-ring N compounds and hydrocarbons with time (25 h on stream), whereas

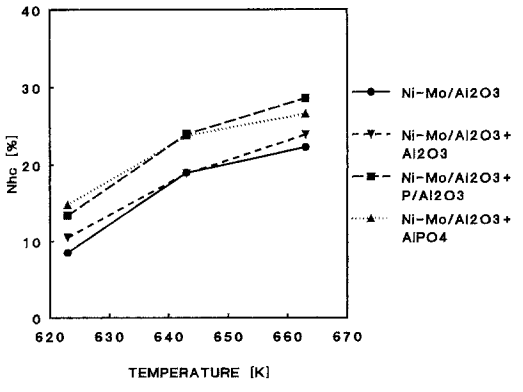

FIG. 6. Quinoline conversion to hydrocarbons, N_{hc} in percentage, versus reaction temperature of *Ni*Mo/Al_2O_3, *Ni*Mo/Al_2O_3 + *P(4)/Al_2O_3, and *Ni*Mo/Al_2O_3 + $AlPO_4$.

TABLE 4

Thiophene HDS (673 K, 0.1 MPa)

Catalyst[a]	Product distribution and reaction rate constants[b]				
	N_{hc}	n_{ba}	k_{hds}	k_{hydr}	k_{hydr}/k_{hds}
*Al_2O_3	0	—	—	—	—
*P(4)/Al_2O_3	0	—	—	—	—
*Ni(1.5)/Al_2O_3	1	—	0.1	—	—
*Ni(1.5)P(4)/Al_2O_3	1	—	0.1	—	—
*Mo/Al_2O_3	6	17	0.6	3.6	5.8
*MoP(4)/Al_2O_3	7	17	0.6	3.6	5.7
*Ni(1.5)Mo/Al_2O_3	50	27	6.6	5.6	0.9
*Ni(1.5)MoP(0.5)/Al_2O_3	49	23	6.4	4.7	0.7
*Ni(1.5)MoP(1)/Al_2O_3	48	22	6.3	4.4	0.7
*Ni(1.5)MoP(2)/Al_2O_3	45	21	5.7	4.3	0.7
*Ni(1.5)MoP(4)/Al_2O_3	44	17	5.6	3.3	0.6
*Ni(1.5)MoP(6)/Al_2O_3	41	16	5.1	3.2	0.6
*Ni(0.5)Mo/Al_2O_3	24	19	2.6	4.0	1.5
*Ni(0.5)MoP(0.5)/Al_2O_3	27	16	3.0	3.5	1.2
*Ni(0.5)MoP(2)/Al_2O_3	29	17	3.3	3.5	1.1
*Ni(0.5)MoP(4)/Al_2O_3	25	13	2.8	2.6	0.9
[Ni(0.6)Mo + NTA]/Al_2O_3	61	20	9.0	3.9	0.4
[Ni(0.6) + NTA]P(2)/Al_2O_3	63	19	9.5	3.5	0.4
*Rh(0.5)/Al_2O_3	9	14	0.9	2.9	3.2
*P(1)*Rh(0.5)/Al_2O_3	10	13	1.0	2.7	2.6

[a] For notation see Catalysts section under Experimental.

[b] N_{hc} is the conversion of thiophene to hydrocarbons (in %); $n_{ba} = N_{ba}/N_{hc}$ is the selectivity for butane (in %), with N_{ba} being the conversion of thiophene into butane (in %); k_{hds} and k_{hydr} are the first-order rate constants for the thiophene conversion to hydrocarbons and the consecutive butene hydrogenation (in 10^{-3} m^3 kg^{-1} s^{-1}).

all Ni–Mo–P/Al_2O_3 catalysts lost about 50% of their N_{hc} during the same period. Phosphate influenced the performance of *Rh(0.5)/Al_2O_3 in a manner similar to that of the Ni–Mo catalysts. N_{hc} and N_{by} increased considerably (Table 2A, 2B), while the selectivity for OPA did not change. Also the apparent activation energy for the *Rh(0.5)/Al_2O_3 catalyst increased in the presence of phosphate. The *Rh(0.5)/Al_2O_3 catalyst had a very high selectivity for PCH (n_{pch}). In the presence of phosphate the selectivity for PCHE (n_{pche}) remained unchanged, that for PCH (n_{pch}) decreased, and that for PBZ (n_{pbz}) increased at constant space time. Just like the Ni–Mo–P/Al_2O_3 catalysts, the *P(1)*Rh(0.5)/Al_2O_3 catalyst had a selectivity slightly higher for DHQ but a THQ1 selectivity lower than that of the corresponding P-free catalyst.

Thiophene HDS

The Al_2O_3 support and *P(4.0)/Al_2O_3 catalyst had no thiophene conversion, while the thiophene conversion and butene hydrogenation of *Ni(1.5)/Al_2O_3 and *Mo/Al_2O_3 were low and did not change with phosphate addition (Table 4). In the *Ni(0.5)MoP(0–4)/Al_2O_3 series the thiophene conversion increased slightly whereas the butene hydrogenation decreased with increasing P-loading. In the *Ni(1.5)MoP(0–6)/Al_2O_3 series

TABLE 5

XPS on Oxidic and Sulfided Catalysts

Catalyst[a]	Intensity ratios[b]							
	Oxidic			Sulfided				
	Ni/Al	Mo/Al	P/Al	Ni/Al	Mo/Al	P/Al	S/Al	S[c]/Al
*Ni(1.5)/Al_2O_3	117	—	—	—	—	—	—	—
*Ni(1.5)P(4)/Al_2O_3	155	—	26	—	—	—	—	—
*Mo/Al_2O_3	—	110	—	—	—	—	—	—
*MoP(4)/Al_2O_3	—	163	23	—	—	—	—	—
*Ni(1.5)Mo/Al_2O_3	115	109	—	72	99	—	30	41
*Ni(1.5)MoP(0.5)/Al_2O_3	90	108	5	86	116	3	40	48
*Ni(1.5)MoP(1)/Al_2O_3	110	118	8	93	127	7	38	52
*Ni(1.5)MoP(2)/Al_2O_3	116	128	15	86	127	12	46	52
*Ni(1.5)MoP(4)/Al_2O_3	100	112	15	98	153	16	43	62
*Ni(0.5)Mo/Al_2O_3	37	103	—	33	127	—	40	48
*Ni(0.5)MoP(0.5)/Al_2O_3	39	114	4	—	—	—	—	—
*Ni(0.5)MoP(2)/Al_2O_3	32	144	13	30	127	10	38	48
*Ni(0.5)MoP(4)/Al_2O_3	56	156	24	35	140	22	40	52
*Rh(0.5)/Al_2O_3	31 (Rh/Al)		—					
*P(1)*Rh(0.5)/Al_2O_3	25 (Rh/Al)		6					

[a] For notation see Catalysts section under Experimental.

[b] For the determination of the XPS intensity ratios see Experimental.

[c] Theoretical S/Al ratios calculated using the experimental Ni/Al and Mo/Al intensity ratios and assuming a NiS and MoS_2 stoichiometry.

there was a decrease in the thiophene conversion and butene hydrogenation with increasing P-loading, but the decrease of k_{hds} is small if a correction is made for the decrease of the metal weight percentages per unit weight of catalyst with increasing P-content. The k_{hydr}/k_{hds} ratio in both series of Ni–Mo–P/Al_2O_3 catalysts decreased with increasing P-loading. For the *Rh/Al_2O_3 catalyst an unchanged k_{hds} and a decreased k_{hydr} were found in the presence of phosphate. Also in the thiophene HDS test, the commercial Ni(1.5)Mo(3)P(2.6)/Al_2O_3 catalyst showed a conversion and selectivity close to those of our Ni(1.5)MoP(2–4)/Al_2O_3 catalysts.

XPS

Oxidic catalysts. The Ni/Al and Mo/Al intensity ratios of the *Ni(1.5)/Al_2O_3 and *Mo/Al_2O_3 catalysts increased strongly in the presence of phosphate (Table 5). Consistent with other results (*9, 13, 14, 18*), the P/Al ratio for loadings below 2 P at. nm^{-2} increased with the P-loading, but levelled off at higher loadings. In contrast to studies which reported a decrease of Mo/Al with increasing P-loading (*9*) or a maximum for the Ni/Al and Mo/Al intensity ratios (*13, 14*), and in contrast to the results of *Ni(1.5)/Al_2O_3 and *Mo/Al_2O_3, the Ni/Al and Mo/Al ratios did not change significantly with P-loading in the *Ni(1.5)MoP(0–6)/Al_2O_3 series. The Ni/Al and Mo/Al intensity ratios of the *Ni(1.5)MoP(1)/Al_2O_3 catalyst were equal to those of a *Ni(1.5)*Mo*P(1)/Al_2O_3 catalyst that was calcined after each impregnation step, and to those of a coimpregnated *[Ni(1.5)MoP(1)]/Al_2O_3 catalyst. This indicates that in all catalysts the Ni and Mo distribution is uniform. In the *Ni(0.5)MoP(0–4)/Al_2O_3

series the Mo/Al intensity ratio increased with P-loading, while the Ni/Al ratio fluctuated strongly but did not follow any distinct trend. The measured Ni/Al and Mo/Al ratios were in all cases lower than the theoretical values calculated for monolayer coverage. The binding energies of the Ni 2*p* and Mo 3*d* peaks did not change with phosphate addition, which, however, does not exclude the possibility of the formation of Ni–P or Mo–P compounds since the differences between the binding energies of metal oxides and metal phosphates are small. No evidence has been found for the formation of phosphides (binding energy difference for P 2*p* about 4 eV). For the *Rh(0.5)/Al_2O_3 catalyst a decrease of the Rh/Al XPS intensity ratio was found in the presence of phosphate.

Sulfided catalysts. Just like in the oxidic catalysts, the P/Al ratios of the sulfidic catalysts were proportional to the P-loading (Table 5). Also the Mo/Al intensity ratio increased with P content, the Ni/Al and the S/Al intensity ratio scattered somewhat and did not follow any distinct trend. All intensity ratios were rather low for the *Ni(1.5)Mo/Al_2O_3 catalysts. The catalyst with the highest P-loading, *Ni(1.5)MoP(6.0)/Al_2O_3, had very high P/Al, Mo/Al, and S/Al ratios. The variation of the Ni/Al and Mo/Al intensity ratios as a function of the P-loading was not quite identical to that of the oxidic catalysts, the Ni/Al ratio was usually somewhat lower, and the Mo/Al ratio somewhat higher compared to the oxidic catalysts. As also reported by Chadwick *et al.* (*9*), the area of the S peaks was in all cases lower than expected based on the Ni/Al and Mo/Al intensity ratios (Table 5). The calculated S deficit (using the Scofield sensitivity factors (*43*)) fluctuated somewhat at low P-loadings and was rather high above 4 P at. nm^{-2}.

Catalyst Texture

The addition of phosphate to Al_2O_3 leads to the formation of $AlPO_4$ and decreases the surface area and pore volume of the Al_2O_3 support to a great extent especially at high P-loadings (*12–16*). Indeed the surface area and pore volume of our Ni–Mo catalysts decreased continuously with increasing P-loading (Table 1). The P-loadings of spent catalysts which had been 32 h on stream were the same as those of the corresponding fresh catalysts, demonstrating that the phosphate, even when present at high concentrations, is strongly bound to the Al_2O_3 support. The loss of surface area and especially pore volume was larger than would be expected based on the decrease of Al_2O_3 content (calculated under the assumption that all phosphate is present as $AlPO_4$ and that neither $AlPO_4$, nor MoO_3 or NiO, contribute to the surface area and pore volume). The discrepancy between the experimental and theoretical values increased with P-loading and is due to the plugging of Al_2O_3 mesopores by $AlPO_4$. In agreement with other studies (*14, 16, 47*), the average pore diameter remained unchanged at low P-loadings (3.3 nm) but increased somewhat at high P-loadings, indicating that the narrow mesopores especially were plugged by phosphate. The high loss of surface area for the catalysts with high P-loading, which might have a negative effect on the distribution of the active phase on the support, had no negative influence on the HDN performance of the catalysts. Apparently this negative effect was overshadowed by positive (physical and chemical) modifications of the active phase.

Phosphate strongly bound to the Al_2O_3 surface in the form of $AlPO_4$ might change the concentration and strength of the acid sites. The results of different studies on this subject are not consistent, predicting a decrease (*8*) or reporting an increase (*14, 16*) of the acidity. In the present study, the acidity of the pure Al_2O_3 and *P(4)/Al_2O_3 samples were measured by NH_3 TPD in the oxidic state. The strong, presumably Lewis, acid sites of the support disappeared after the addition of phosphate, but the total amount of adsorbed NH_3 was approxi-

mately the same for both samples, i.e., 0.6 mmol g^{-1}.

The *P(4)/Al_2O_3 catalyst had a negligible Q-conversion to hydrocarbons (N_{hc}) but its Q-cracking and isomerisation (N_{by}) was somewhat increased compared to the Al_2O_3 support (see Table 2A, 2B). The analysis of some of our spent Ni–Mo–P/Al_2O_3 catalysts showed that the coke formed in the P-containing catalysts had a higher H/C ratio and was more reactive than the coke in the P-free catalysts (J. van Doorn, unpublished results). The changes of the Q-cracking and isomerisation (N_{by}) and coking propensity are related to acid properties (*8, 11*) and do not necessarily have to correspond to the changes in HDS and HDN activities.

DISCUSSION

The HDN experiments demonstrate that the addition of Ni to Mo/Al_2O_3 and the addition of phosphate to Ni–Mo/Al_2O_3, Ni–Mo(NTA)/Al_2O_3, and Rh/Al_2O_3 catalysts significantly increase the conversion of Q to hydrocarbons. Simultaneously the PCH and PBZ selectivities and the apparent activation energy change. On the other hand, although the thiophene conversion of Mo/Al_2O_3 is increased by Ni, the thiophene conversion of Ni–Mo/Al_2O_3, Ni–Mo(NTA)/Al_2O_3, and Rh/Al_2O_3 catalysts is almost unaffected by phosphate; only the butene hydrogenation decreases. Also the thiophene HDS activity of Fe–Mo/Al_2O_3 and Co–Mo/Al_2O_3 catalysts were unaffected by phosphate (*48*). These observations cannot be explained by a mere increase of the number of Ni–Mo and Rh catalytic sites by P without changing (part of) the sites, since then HDN as well as HDS conversions should have increased and there should have been one general selectivity curve instead of different curves for each P-loading (Fig. 4). In accordance with these catalytic results, we could find no simple correlation between the Ni and Mo dispersion, or the S deficit, and the HDN (and HDS) conversion, although the XPS results on oxidic and sulfidic catalysts show that phosphate influences the distribution of the metals on the Al_2O_3 support. Apparently the changes of the catalytic performance of these catalysts cannot be explained only by the changes of the dispersion of the active phase. Also since the apparent HDN activation energies change with P-loading and both in HDN and HDS the saturates/unsaturates ratio decreases with increasing P-loading for both the Ni–Mo and Rh catalysts, we conclude that P introduces new catalytic sites or changes the existing sites.

It is well known that phosphate weakens the interaction between Mo and the Al_2O_3 support (*15*) and therefore phosphate may be expected to increase the sulfidability of the oxidic Mo phase, to decrease the Mo dispersion, and to induce the formation of the Ni–Mo–S type II structure. Originally Candia *et al.* defined the type II structure as that Co–Mo–S structure which after sulfidation at high temperature has a high intrinsic activity and suggested that while the type I structure is characterised by interactions between the Co–Mo–S phase and the support via Mo–O–Al linkages, type II might have few if any such linkages (*25*). In subsequent studies Vissers *et al.* suggested that the high HDS activity of carbon-supported hydrodesulfurisation catalysts was due to the presence of Co–Mo–S II, because of the weak catalyst–carbon interaction (*21*), and van Veen *et al.* assumed that the high activity obtained with a Co–Mo catalyst prepared in the presence of a complexing agent like nitrilotriacetic acid (NTA) was due to the prevention of the catalyst–support interaction leading to the preferential formation of the type II structure (*23*). The Co atoms in the Co–Mo–S phase of the NTA-prepared catalyst were found to have twice the HDS activity as the Co atoms in the Co–Mo–S phase present in a classically prepared catalyst, which was supposed to consist mainly of type I Co–Mo–S (*49*). This factor of two is in good agreement with the factor ob-

served by Candia *et al.* (*25*). For Co–Mo/Al_2O_3 catalysts prepared in the presence of phosphate van Veen *et al.* observed a linear relationship between k_{hds} and the amount of Co in the Co–Mo–S phase (as determined by Mössbauer spectroscopy) with a slope intermediate between those of the NTA-prepared and classic Co–Mo catalysts, indicating that phosphate-containing Co–Mo/Al_2O_3 catalysts contain a mixture of type I and type II Co–Mo–S structures (*49*).

Whether in all cases it is possible to subdivide the Co(Ni)–Mo–S phase into two types is, of course, a moot point. Type II, the fully sulfided form with no interactions with the support, appears to be relatively well defined, but type I is certainly less well defined, as the number of Mo–O–Al (or Ni–O–Al) linkages is unknown and is likely to vary with sulfidation and reaction conditions. The Ni and/or Ni–Mo sites in type I which are not linked to the support might have the same intrinsic activity as in type II, since the electronic effects of linkages to the support are most probably very local. The fact that the type II structure has been observed to have about twice the intrinsic activity per Co (or Ni) atom in the Co–Mo–S (or Ni–Mo–S) structure as that in the type I structure cannot be due to half of the Co or Ni atoms being linked via one or two oxygen atoms to the support, because in that case Co–O and Ni–O coordinations should have been easily observed in EXAFS. Since this is not the case (*50, 51*), the number of such linkages should be small in comparison to the number of Co or Ni atoms around the MoS_2 edge. This only leaves the possibility that type I is less active than type II because of steric reasons. It might be that because of blockage by the support, in type I the reactants cannot approach those sites which are close to the Mo–O–Al linkages. It is an open question whether this means that type II Ni–Mo–S structures are parallel to the Al_2O_3 surface and type I are standing up (*52*), or that type II is a multistacked structure and type I a monolayer structure (*24*).

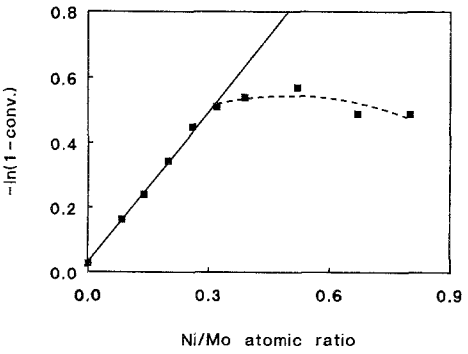

FIG. 7. Thiophene HDS activity of Ni–Mo(8.3%)P(1.9%)/Al_2O_3 catalysts as a function of the Ni/Mo atomic ratio.

Let us investigate whether our results can be explained with changes in the proportions of type I and II in our catalysts. In the Ni(0.5) series of catalysts the ratio Ni/Mo = 0.24 is low enough for all Ni to end up in the Ni–Mo–S phase. This expectation is based on ^{57}Co Mössbauer emission spectroscopic work on the analogous Co–Mo system (*49, 53*) and on the results of an EXAFS investigation of a series of Ni–Mo catalysts, which showed that at a Mo loading of about 7% Ni_3S_2 could only be observed for Ni/Mo > 0.5 (*54*). This expectation is also corroborated for Ni–Mo–P/Al_2O_3 catalysts. As shown in Fig. 7, the thiophene HDS performance of a number of Ni–Mo–P/Al_2O_3 catalysts with fixed Mo and P loading increases linearly with Ni loading up to Ni/Mo = 0.35. We therefore compare catalyst activities normalised for their Ni contents. The first-order specific rate constants for the HDS of thiophene and the zero-order specific rate constants of the HDN of quinoline (which we checked to be of zero order), per atom of Ni(Rh) per square nanometer of support area, of the Ni(0.5) Mo P(0 and 2), Ni(1.5) Mo P(0 and 2), Ni(0.6) Mo (+NTA) P(0 and 2), and of the Rh(0.5)P(0 and 1) catalysts are presented in Table 6. These specific rate constants k' were obtained from the HDN conversions given in Table 2 and from the HDS rate constants k given in Table 4 by multiplication by the factors 1/0.5, 1/1.5,

TABLE 6

First-Order Thiophene HDS Specific Rate Constants and Zero-Order Quinoline HDN-Specific Rate Constants per Atom Ni(Rh) per Square Nanometers Support Surface Area

	k'_{hds}	k'_{hdn}
Ni(0.5)Mo	5.2	0.25
Ni(0.5)MoP(2)	7.2	0.48
Ni(1.5)Mo	4.4	0.16
Ni(1.5)MoP(2)	4.0	0.30
Ni(0.6)Mo + NTA	15	0.56
[Ni(0.6)Mo + NTA]P(2)	16	1.15
Rh(0.5)	1.8	0.36
Rh(0.5)P(1)	2.0	0.58

1/0.6, and 1/0.5 for the Ni(0.5)MoP(0, 2), Ni(1.5)MoP(0, 2), [Ni(0.6)Mo + NTA] P(0, 2), and Rh(0.5)P(0, 1) catalysts, respectively. A further correction factor of 1.2/1.1 was applied to the rate constants for the Ni(0.5)MoP catalyst and a factor of 7.7/7.3 for the Ni(1.5)MoP(2) catalyst, to correct for the fact that the activities presented in Tables 2 and 3 were determined per gram of catalyst (cf. Table 1). Comparison of the Ni(0.5)Mo and Ni(0.6)Mo + NTA results shows that, as observed for Co–Mo catalysts (*23*), for Ni–Mo also the addition of NTA during catalyst preparation enhances the HDS activity appreciably. For the first time it is shown that for HDN also the NTA-based catalysts are much more active than catalysts prepared via conventional routes. If it is assumed that the NTA-based Ni(0.6)Mo catalyst consists of type II Ni–Mo–S and the conventionally prepared Ni(0.5)Mo catalyst of type I, then it can be concluded that type II is 2.9 times more active in HDS and 2.3 more active in HDN than type I. Implicit in this is the reasonable assumption that the activity of Ni–Mo–S structures is dominated by the activity of the Ni-containing sites (cf. Fig. 7).

If the only effect of phosphate in the Ni–Mo catalysts was to influence the proportion of type I and type II, then the HDS and HDN activities of the Ni(0.5)Mo catalyst should increase upon phosphate addition, since the strong phosphate–alumina interaction can only decrease the molybdate–alumina interaction and thus, after sulfidation, increase the proportion of the type II structure. Even if an increase in the MoS_2 crystallite size of the Ni–Mo–S phase(s) would occur, this would not lead to Ni_3S_2 segregation and to a decrease of specific activity, because of the low Ni/Mo = 0.24 ratio. The total number of Ni–Mo–S sites would stay constant, but the proportion of type II would increase upon phosphate addition. On the other hand, phosphate should have no influence on the NTA-prepared Ni(0.6)Mo catalyst, since in that catalyst all Ni should already be in the most active Ni–Mo–S II form. Although k'_{hds} and k'_{hdn} for the Ni(0.5)Mo catalyst indeed increase upon phosphate addition and k'_{hds} for the Ni(0.6)Mo + NTA catalyst stays more or less constant, k'_{hdn} of the NTA catalyst is doubled by the phosphate addition (Table 6). This suggests that, although the type I to II structure transformation may explain part of the results, it cannot explain all, especially not the HDN results. This special position of the HDN results is also evident in the other catalysts. Phosphate influences the performance of the Rh catalyst in a way similar to that of the Ni–Mo + NTA, or indeed to all Ni–Mo, catalysts. The HDN activity is improved considerably, while the HDS activity is not influenced much. Since rhodium sulfide has a crystal structure completely different than that of MoS_2, it is hard to believe that a type I to II structure transformation also plays a role for rhodium sulfide. This means that the increase in HDN conversion upon phosphate addition, which was observed in all catalyst systems studied, must be inherent to the mechanism of the HDN of quinoline.

The HDN and HDS reaction networks are complex, rather than simple single-step, reaction networks. In the Q–HDN network hydrogenation as well as N-removal (elimination and/or hydrogenolysis) reactions are present (*27–35*) (cf. Fig. 1). These reactions occur on different sites, as demonstrated by

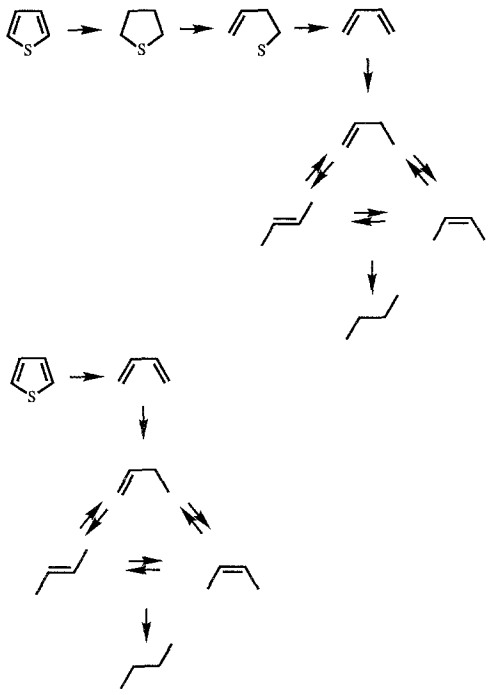

FIG. 8. Two reaction networks proposed for the HDS of thiophene.

the fact that addition of H_2S during HDN decreases ring hydrogenation activity and increases aliphatic C–N bond breaking (*30, 32*). Yang and Satterfield assumed (*55*) that the former reactions take place on Mo cations with a sulphur vacancy, while the latter reactions take place on Brønsted acid sites, originating from H_2S adsorption on the metal sulfide (*56*), from the support, or from the phosphate promoter. We may add that hydrogenation may also take place on Ni or Ni–Mo–S sites. A HDN catalyst might thus rightly be called a bi- or even a polyfunctional catalyst. The work of Shih *et al.* (*27*) and Satterfield *et al.* (*31, 33*) shows that in the HDN of Q the N-removal from DHQ as well as the preceding hydrogenations are slow steps, thus precluding a rate-determining-step treatment. The thiophene HDS reaction network is still under debate (*57*). It seems certain that at high pressure the mechanism is similar to that of HDN (*35*), hydrogenation followed by S-removal (Fig. 8). The reaction at 1 atm may, however, take place via the direct hydrogenolysis of thiophene to butadiene, followed by hydrogenation to butene and butane, or via the high-pressure mechanism (*58*). There is general agreement, however, that the first step—be it the hydrogenation or the hydrogenolysis of thiophene—is rate determining. This first step is assumed to take place on a Mo, Ni, or Ni–Mo–S site, which has a sulphur vacancy.

We can suggest three explanations for the special effect of phosphate on the HDN of quinoline. First, there might be a support effect, with phosphated alumina inducing a structural change in the Ni–Mo–S phase or affecting it electronically. It is not immediately apparent, however, why this should lead to a large change in HDN activity, while leaving the HDS activity virtually unaffected. Another possibility is that phosphate enhances the adsorption of quinoline, or influences the manner in which it is adsorbed. Space velocity variations suggest, however, that the order in quinoline is close to zero, in which case one should not expect a large effect of phosphate on the strength of adsorption. Only if the adsorption geometry of the double-ring N compounds is changed by the presence of phosphate, for instance if adsorption takes place on adjacent Ni–Mo–S and PO_4 sites, can the rate constant change even though the order stays zero in quinoline. A third possibility is that in the Q–HDN dual-site mechanism phosphate provides (extra) N-removal (elimination and or hydrogenolysis) sites. After all, pure Al_2O_3 is already a good catalyst for the denitrogenation of piperidine and other cyclic amines (*59*).

To find out whether the effect of phosphate was due to the catalytic activity of $AlPO_4$ formed on the Al_2O_3 support, experiments with dual beds were done. The idea behind the dual bed experiments is that the product mixture of the *Ni*Mo/Al_2O_3 catalyst bed, which contains hydrogenated intermediates like OPA and DHQ that can undergo N-removal, is brought into contact with the second (downstream) catalyst bed. In this way one can check whether a mate-

rial, which itself has no hydrogenation activity and cannot form these intermediates but is able to denitrogenate them, contributes to the overall Q-conversion to hydrocarbons. The dual bed experiments proved that phosphate-containing supports are indeed capable of catalysing some of the steps in the Q–HDN reaction network. *P(4)/Al_2O_3 and $AlPO_4$ have negligible Q-conversions to hydrocarbons, but used as after beds they increased the Q-conversion to hydrocarbons. PCH contributes most to the increased hydrocarbon production and judged from the data presented in Table 3 this is mainly due to an increased conversion of DHQ. This indicates that the P-containing Al_2O_3-supported Ni–Mo catalysts might be bifunctional. The metal sulfides not only provide hydrogenation sites necessary to form alicyclic intermediates, but also sites for aliphatic C–N bond breaking and N-removal as demonstrated by the good HDN properties of carbon-supported metal sulfides (*45–48*). $AlPO_4$ provides additional sites for C–N bond breaking and N-removal.

The bifunctional model also explains why phosphate had only a minor effect on the HDN performance of the *Ni/Al_2O_3 and *Mo/Al_2O_3 catalysts. These catalysts clearly had an insufficient hydrogenation activity, which cannot be remedied by phosphate. The hydrogenation activity of the *Ni(0.5)Mo/Al_2O_3 catalysts is much better than that of *Mo/Al_2O_3, so that hydrogenation is no longer rate determining, and phosphate can have a beneficial influence. The negligible influence of phosphate on the HDS of thiophene at 1 atm, on the other hand, is due to the fact that the step preceding the sulphur removal is rate determining. If the HDS of thiophene takes place via direct hydrogenolysis, only a metal sulfide and no phosphate is required for hydrogenolysis, and also if thiophene is desulfurised by hydrogenation and subsequent S-elimination, the first reaction step is rate determining, since even in the absence of phosphate no tetrahydrothiophene is observed (*57, 58*). Also in that case phosphate will have no influence.

Diez *et al.* recently observed in coking studies of Ni–Mo–P/Al_2O_3 catalysts that the rate constants for hydrogenation and N-removal in the HDN of quinoline both decreased upon coking, but that the rate constant for N-removal decreased more strongly (*60*). This confirms that the N-removal reaction takes (at least partly) place at sites other than the hydrogenation sites and that the Ni–Mo–P/Al_2O_3 HDN catalyst is bifunctional. Although we have not yet performed a kinetic investigation of the reaction network of the HDN of quinoline with and without phosphate, our preliminary results are in qualitative agreement with the findings of Diez *et al.* At constant space time the selectivities n_{dhq} and n_{thq5} in the group of N-containing heterocycles were lower for the P-containing *Ni(1.5)Mo catalysts than for the P-free catalyst, indicating that the N-removal rate increased relative to the hydrogenation rate.

Having explained why phosphate influences the HDN rate but not the HDS rate, we can quantitatively analyse the data of Table 6. Because of their low Ni/Mo ratio the Ni(0.5)Mo and Ni(0.6)Mo NTA catalysts, with or without phosphate, contain no Ni_3S_2. Under the assumption that the NTA-based catalysts contain Ni exclusively in the Ni–Mo–S II form, one calculates that k'_{hds} (Ni–Mo–S II) = 15.5, k'_{hdn} (Ni–Mo–S II) = 0.56 and k'_{hdn} (Ni–Mo–S II + P) = 1.15. Substituting these values in the equations for the Ni(0.5)Mo catalyst,

$$\alpha k'_{hds}(\text{Ni–Mo–S I}) + (1 - \alpha)k'_{hds}(\text{Ni–Mo–S II}) = 5.2$$

$$\alpha k'_{hdn}(\text{Ni–Mo–S I}) + (1 - \alpha)k'_{hdn}(\text{Ni–Mo–S II}) = 0.25,$$

and

$$\alpha' k'_{hds}(\text{Ni–Mo–S I}) + (1 - \alpha')k'_{hds}(\text{Ni–Mo–S II}) = 7.2$$

$$\alpha' k'_{hdn}(\text{Ni–Mo–S I + P}) + (1 - \alpha')k'_{hdn}(\text{Ni–Mo–S II + P}) = 0.48$$

for the Ni(0.5)MoP(2) catalyst, one obtains $0.72 \leq \alpha \leq 1.0$ and $\alpha'/\alpha = 0.81$, in which α

and α' are the fractions of Ni in the Ni–Mo–S I form in the Ni(0.5)Mo and Ni(0.5)MoP(2) catalysts, respectively. In view of the high calcination temperature of 823 K it is reasonable to assume that all Ni–Mo–S in the Ni(0.5)Mo catalyst is in the Ni–Mo–S I form. With $\alpha = 1.0$, α' becomes equal to 0.81, substantiating that phosphate increases the proportion of Ni–Mo–S in the II form. With $\alpha = 1.0$ and $\alpha' = 0.81$ one also calculates that k'_{hds}(Ni–Mo–S I) = 5.2, k'_{hdn}(Ni–Mo–S I) = 0.25 and k'_{hdn}(Ni–Mo–S I + P) = 0.32.

Having obtained the intrinsic HDS and HDN rate constants for the Ni–Mo–S I and II phases, with and without phosphate, we can analyse the results for the Ni(1.5)Mo and Ni(1.5)MoP catalysts. The Ni/Mo atomic ratio of these catalysts is quite high (0.72), so that they contain more Ni than can be accommodated in the Ni–Mo–S phase (see the above discussion on the Ni/Mo limit in the Ni–Mo–S phase). This means that in the sulfided state these catalysts contain nickel sulfide in addition to Ni–Mo–S. This nickel sulfide phase, like the cobalt sulfide phase in Co–Mo catalysts (*53*), may be assumed to have a negligible activity relative to the Ni–Mo–S phase(s). This directly explains why the Ni(1.5)Mo catalysts have lower specific rate constants than the Ni(0.5)Mo catalysts (Table 6). Another point is that the type II MoS_2 crystallites are larger than the type I crystallites (*49*), since the former type is generated from molybdenum oxide in weak interaction with the support. As a consequence, the more type II is present, the more Ni will be forced to segregate as nickel sulfide (presumably Ni_3S_2 (*54*)). In the P-containing catalysts not only the interaction between molybdate and support will be weaker, but also, because phosphate decreases the support surface area (cf. Table 1), a greater extent of formation of bulk MoO_3 and polymeric molybdenum oxide will occur, which after sulfiding leads to larger MoS_2 crystallites with less interaction with the support (*61*). Thus Fierro *et al.* observed a decrease in the intensity of the 1791 cm^{-1} IR band of NO adsorbed on sulfided Mo/Al_2O_3 by a factor of 4 when phosphate was present (*62*).

With only Ni–Mo–S I and II contributing to the HDS and HDN activities it should have been possible to evaluate their contributions in the Ni(1.5)Mo and Ni(1.5)MoP(2) catalysts from the specific HDS and HDN rate constants given in Table 6. Unfortunately, however, for both catalysts the two equations for k'_{hds} and k'_{hdn} turned out to be correlated and the Ni fractions in the Ni–Mo–S I and II phases could not be determined uniquely. The Ni(1.5)Mo composition can be anywhere between 0.75 I + 0.25 Ni_3S_2 and 0.28 II + 0.72 Ni_3S_2, while the Ni(1.5)MoP(2) composition should be between 0.85 I + 0.15 Ni_3S_2 and 0.26 II + 0.74 Ni_3S_2. But from the data in Tables 2 and 3 it appears that Ni(1.5)Mo/Al_2O_3 is about twice as active in the HDS of thiophene and HDN of quinoline as its Ni(0.5)Mo/Al_2O_3 counterpart, which suggests that about two-thirds of the Ni in the sulfided Ni(1.5)Mo catalyst is present as Ni–Mo–S I. This estimate would limit the Ni/Mo ratio in the Ni–Mo–S phase to 1/2.1 = 0.5 and would be in agreement with the EXAFS investigation on Ni–Mo/Al_2O_3 and Ni–Mo/C catalysts, in which segregated Ni_3S_2 was only observed for Ni/Mo > 0.5 (*54*). The presence of phosphate in the Ni(1.5)MoP(2)/Al_2O_3 catalyst decreases the specific HDS rate constant slightly, which can only be explained by a loss of the Ni dispersion, and thus by a decrease in the Ni–Mo–S edge area and an increase in the amount of Ni_3S_2. When, as to be expected from the increased HDN rate constant, the phosphate induces (partly) the formation of Ni–Mo–S II, then the loss of Ni dispersion should be even greater, to compensate for the larger activity of Ni sites in the Ni–Mo–S II phase. Reasonable possibilities for the compositions of the Ni(1.5)Mo and Ni(1.5)MoP(2) catalysts would thus be 0.6 I + 0.07 II + 0.33 Ni_3S_2 and 0.2 I + 0.2 II + 0.67 Ni_3S_2, respectively.

Because of the difference in sulfidation in the HDS and HDN cases and of the uncertainty in the conversion measurements, and

also because of possible differences in the (small) amounts of Ni lost to the support (as nickel aluminate spinel), the calculated fractions of the Ni–Mo–S I and II and Ni_3S_2 phases should be used qualitatively, rather than quantitatively. These fractions will furthermore depend on the preparation (calcination and sulfidation) and testing conditions. Nevertheless, it is clear that the effect of phosphate is due to a combination of factors. On the one hand, in the presence of phosphate the structure and dispersion of nickel are changed. Ni–Mo–S II is formed at the expense of Ni–Mo–S I, but the dispersion of MoS_2 decreases and leads, at high Ni loadings, to Ni_3S_2 segregation. The formation of Ni–Mo–S II is beneficial, because its HDS and HDN activities are higher than those of Ni–Mo–S I. But the Ni_3S_2 segregation is, of course, counterproductive. On the other hand, phosphate can play a direct role in the catalysis. For the HDS of thiophene at 1 atm this role is unimportant, but for the HDN of quinoline it gives an additional factor of about two in activity. For HDS these three factors lead to a somewhat higher activity for phosphate containing Ni–Mo catalysts with low Ni loading, but to a slightly smaller activity at high Ni loading. For the HDN of quinoline they lead to an increased activity of phosphate-containing Ni–Mo catalysts at all Ni loadings.

CONCLUSIONS

Phosphate is an efficient HDN promoter in the nitrogen removal from quinoline over Ni–Mo/Al_2O_3 and Rh/Al_2O_3 catalysts, but does not significantly influence the sulphur removal from thiophene. The effect of phosphate is due to a combination of several factors. On the one hand phosphate improves the catalytic properties, both for HDN and HDS, by promoting the formation of the type II Ni–Mo–S phase. On the other hand, phosphate leads to growth of the Ni–Mo–S crystallites, which, especially at high Ni loading, leads to the segregation of Ni_3S_2 and loss of activity. In addition to these structural effects, phosphate plays a direct role in the HDN reaction, since the removal of nitrogen from cyclic amines is promoted by phosphate. Although both the HDN and the HDS reactions are dual functional, only the HDN reaction is promoted by phosphate, because in the HDS of thiophene at 1 atm the hydrogenation or hydrogenolysis, preceding the S-removal step, is rate determining.

As a general rule for both HDN and HDS it can thus be stated that the effect of phosphate depends on whether the C–S or C–N bond-breaking steps are slower or faster than the hydrogenation steps. Thus, in the HDN of quinoline (with its slow N-removal from DHQ) phosphate has a beneficial effect, in the HDS of thiophene it has no effect, and in the HDN of pyrrole, in which the first hydrogenation step is rate determining (*35*), it is predicted to have no effect. Phosphate therefore has an effect similar to that of H_2S, which accelerates C–N bond breaking and slows down hydrogenation (*30, 32, 63*) and thus accelerates the HDN of quinoline (*30, 32*) and decelerates the HDN of pyrrole (*64*) and the HDS of thiophene.

ACKNOWLEDGMENTS

These investigations were supported by the Netherlands Foundation for Chemical Research (SON) with financial aid from the Netherlands Technology Foundation (STW). The authors thank A. Elemans-Mehring for the analysis of the catalysts, M. Mittelmeijer-Hazeleger (University of Amsterdam) for the BET measurements, and A. Heeres (University of Groningen) for assistance in the XPS analysis of the sulfided samples.

REFERENCES

1. Morales, A. L., Guillen, J. A. S., De Agudelo, M. M., Martinez, N. P., and Carrasquel, A. R., US Pat. 4,600,703 (1986).
2. Chao, T. H., US Pat. 4,629,717 (1986).
3. Basila, M. R., Feistel, G. R., and Clements, P., Ger. Pat. 2,628,531 (1976); Shell, D. C., and Hayward, E. C., US Pat. 4,024,048 (1977); Nevitt, T. D., US Pat. 4,381,993 (1983); Wilson, G., and Kayamoto, M., US Pat. 4,388,222 (1983); Millman, W. S., US Pat. 4,392,985 (1983); Simpson, H.D., and Richardson, R. L., US Pat. 4,446,248 (1984).
4. Morales, A. L., Galiasso, R. E., Agudelo, M. M.,

Salazar, J. A., and Carrasquel, A. R., US Pat. 4,520,128 (1985).
5. Brown, S. M., and Wallace, D. N., US Pat. 3,969,273 (1976); Ryan, R. C., Adams, C. F., and Washecheck, D. M., US Pat. 4,530,911 (1985).
6. Prins, R., de Beer, V. H. J., and Somorjai, G. A., *Catal. Rev. Sci. Eng.* **31,** 1 (1989).
7. Mickelson, G. A., US Pat. 3,749,663; 3,749,664; 3,755,148; 3,755,150; and 3,755,196 (1973); Pine, L. A., US Pat. 4,003,828 (1975); Miller, J. T., Eur. Pat. 112,667 (1984).
8. Fitz, C. W., and Rase, H. F., *Ind. Eng. Chem. Prod. Res. Dev.* **22,** 40 (1983).
9. Chadwick, D., Aitchison, D. W., Badilla-Ohlbaum, R., and Josefsson, L., *Stud. Surf. Sci. Catal.* **16,** 323 (1982).
10. Hopkins, P. D., and Meyers, B. L., *Ind. Eng. Chem. Prod. Res. Dev.* **22,** 421 (1983).
11. Tischer, R. E., Narain, N. K., Stiegel, G. J., and Cillo, D. L., *Ind. Eng. Chem. Res.* **26,** 422 (1987).
12. Okamoto, Y., Gomi, I., Mori, Y., Imanaka, T., and Teranishi, S., *React. Kinet. Catal. Lett.* **22,** 417 (1983).
13. Atanasova, P., Halachev, T., Uchytil J., and Kraus, M., *Appl. Catal.* **38,** 235 (1988).
14. Ramirez de Agudelo, M. M., and Morales, A., *in* "Proceedings, 9th International Congress on Catalysis, Calgary, 1988" (M. J. Philips and M. Ternan, Eds.), p. 42, Vol. I. Chem. Institute of Canada, Ottawa 1988.
15. Gishti, K., Iannibello, A., Marengo, S., Morelli, G., and Titarelli, P., *Appl. Catal.* **12,** 381 (1984).
16. Morales, A., Ramirez de Agudelo, M. M., and Hernandez, F., *Appl. Catal.* **41,** 261 (1988).
17. Haller, G., McMillan, B., and Brinen, J., *J. Catal.* **97,** 243 (1986); *Div. Petr. Chem. Am. Chem. Soc.* **29,** 939 (1984).
18. Lopez Cordero, R., Gil Llambias, F. J., Palacios, J. M., Fierro, J. L. G., and Lopez Agudo, A., *Appl. Catal.* **56,** 197 (1989).
19. van Veen, J. A. R., Hendriks, P. A. J. M., Andrea, R. R., Romers, E. J. G. M., and Wilson, A. E., *J. Phys. Chem.* **94,** 5275, 5282 (1990).
20. Massoth, F. E., Muralidhar, G., and Shabtai, J., *J. Catal.* **85,** 44, 53 (1984).
21. Vissers, J. P. R., Scheffer, B., de Beer, V. H. J., Moulijn, J. A., and Prins, R., *J. Catal.* **105,** 277 (1987).
22. Duchet, J. C., van Oers, E. M., de Beer, V. H. J., and Prins, R., *J. Catal.* **80,** 386 (1983).
23. van Veen, J. A. R., Gerkema, E., van der Kraan, A. M., and Knoester, A., *J. Chem. Soc. Chem. Commun.*, 1684 (1987).
24. Kemp, R. A., Ryan, R. C., and Smegal, J. A., *in* "Proceedings, 9th International Congress on Catalysis, Calgary, 1988" (M. J. Philips and M. Ternan, Eds.), p. 128, Vol. I. Chem. Institute of Canada, Ottawa 1988.
25. Candia, R., Sørensen, O., Villadsen, J., Topsøe, N.-Y., Clausen, B. S., and Topsøe, H., *Bull. Soc. Chim. Belg.* **93,** 763 (1984).
26. Topsøe, H., and Clausen, B. S., *Appl. Catal.* **25,** 273 (1986).
27. Shih, S. S., Katzer, J. R., Kwart, H., and Stiles, A. B., *Div. Petr. Chem. Am. Chem. Soc.* **22,** 919 (1977).
28. Cocchetto, J. F., and Satterfield, C. N., *Ind. Eng. Chem. Process Des. Dev.* **20,** 49 (1981).
29. Satterfield, C. N., and Cocchetto, J. F., *Ind. Eng. Chem. Process Des. Dev.* **20,** 53 (1981).
30. Satterfield, C. N., and Gultekin, S., *Ind. Eng. Chem. Process Des. Dev.* **20,** 62 (1981).
31. Satterfield, C. N., and Yang, S. H., *Ind. Eng. Chem. Process Des. Dev.* **23,** 11 (1984).
32. Yang, S. H., and Satterfield, C. N., *Ind. Eng. Chem. Process Des. Dev.* **23,** 20 (1984).
33. Satterfield, C. N., and Smith, C. M., *Ind. Eng. Chem. Process Des. Dev.* **25,** 942 (1986).
34. Gioia, F., and Lee, V., *Ind. Eng. Chem. Process Des. Dev.* **25,** 918 (1986).
35. Schulz, H., Schon, M., and Rahman, N. M., *Stud. Surf. Sci. Catal.* **27,** 201 (1986).
36. Geneste, P., Moulinas, C., and Olive, J. L., *J. Catal.* **105,** 254 (1987).
37. Sonnemans, J., Neyens, W. J., and Mars, P., *J. Catal.* **34,** 230 (1974).
38. Ledoux, M. J., Bouassida, A., and Benazouz, R., *Appl. Catal.* **9,** 41 (1984).
39. Campelo, J. M., Marinas, J. M., Mendioroz, S., and Pajares, J. A., *J. Catal.* **101,** 484 (1986).
40. van Veen, J. A. R., and Colijn, H. A., in press.
41. Vrinat, M. L., *Appl. Catal.* **6,** 137 (1983).
42. Bouwens, S. M. A. M., Vissers, J. P. R., de Beer, V. H. J., and Prins, R., *J. Catal.* **112,** 401 (1988).
43. Scofield, J. H., *J. Electron. Spectrosc.* **18,** 129 (1976).
44. Kovach, S. M., Castle, L. J., Bennett, J. V., and Schrodt, J. T., *Ind. Eng. Chem. Prod. Res. Dev.* **17,** 62 (1978).
45. Eijsbouts, S., de Beer, V. H. J., and Prins, R., *J. Catal.* **127,** 619 (1991); **109,** 217 (1988).
46. Eijsbouts, S., Sudhakar, C., de Beer, V. H. J., and Prins, R., *J. Catal.* **127,** 605 (1991).
47. Spojakina, A., Damyanova, S., Petrov, L., and Vit, Z., *Appl. Catal.* **56,** 163 (1989).
48. Bouwens, S. M. A. M., van der Kraan, A. M., de Beer, V. H. J., and Prins, R., *J. Catal.* **128,** 559 (1991).
49. van Veen, J. A. R., Gerkema, E., van der Kraan, A. M., Hendriks, P. A. J. M., and Beens, H., in press.
50. Bouwens, S. M. A. M., Koningsberger, D. C., de Beer, V. H. J., Louwers, S. P. A., and Prins, R., *Catal. Lett.* **5,** 273 (1990).
51. van Dijk, M. P., van Veen, J. A. R., Bouwens,

S. M. A. M., van Zon, F. B. M., and Koningsberger, D. C., *in* "Proceedings, 2nd European Conference on Progress in X-Ray Synchrotron Radiation Research" (A. Balerna, E. Bernieri, and S. Mobilio, Eds.), p. 139. SIF, Bologna, 1990.
52. Hayden, T. F., and Dumesic, J. A., *J. Catal.* **103,** 366 (1987).
53. Wivel, C., Candia, R., Clausen, B. S., Mørup, S., and Topsøe, H., *J. Catal.* **68,** 453 (1981).
54. Louwers, S. P. A., and Prins, R., *J. Catal.* in press.
55. Yang, S. H., and Satterfield, C. N., *J. Catal.* **81,** 168 (1983).
56. Topsøe, N.-Y., Topsøe, H., and Massoth, F. E., *J. Catal.* **119,** 252 (1989).
57. Markel, E. J., Schrader, G. L., Sauer, N. N., and Angelici, R. J., *J. Catal.* **116,** 11 (1989).
58. Zdrazil, M., *Appl. Catal.* **4,** 107 (1982).
59. Ledoux, M. J., and Sedrati, M., *J. Catal.* **83,** 229 (1983).
60. Diez, F., Gates, B. C., Miller, J. T., Sajkowski, D. J., and Kukes, S. G., *Ind. Eng. Chem. Res.* **29,** 1999 (1990).
61. Lopez Cordero, R., Esquivel, N., Lazaro, J., Fierro, J. L. G., and Lopez Agudo, A., *Appl. Catal.* **48,** 341 (1989).
62. Fierro, J. L. G., Lopez Agudo, A., Esquivel, N., and Lopez Cordero, R., *Appl. Catal.* **48,** 353 (1989).
63. Perot, G., Brunet, S., and Hamze, N., *in* "Proceedings, 9th International Congress on Catalysis, Calgary, 1988" (M. J. Phillips and M. Ternan, Eds.), p. 19, Vol. I. Chem. Institute of Canada, Ottawa 1988.
64. Topsøe, H., Clausen, B. S., Topsøe, N.-Y., and Zeuthen, P., *Stud. Surf. Sci. Catal.* **53,** 77 (1990).